

Path Planning of Airfoil Surface for Robotic Fibre Placement

Lina Li, Xingang Wang, De Xu

Research Center of Precision Sensing and Control
Institute of Automation, Chinese Academy of Sciences
Beijing 100190, China
{lilina2013, xingang.wang, de.xu}@ia.ac.cn

Min Tan

The State Key Laboratory of Management and Control for
Complex Systems
Institute of Automation, Chinese Academy of Sciences
Beijing 100190, China
min.tan@ia.ac.cn

Abstract—In this paper, a new path planning algorithm based on triangular meshes of the airfoil open surface for four commonly used laying angles in robotic fibre placement is presented. In the proposed algorithm, the 0° paths are computed by the slicing method, the $\pm 45^\circ$ paths are obtained by general rotation transformation, and the method to equally divide arc is adopted to get the 90° paths which can ensure that the complete fibre tows distributed evenly on the surface connect the root and tip part. Then the redundant path points are deleted, the final path points are obtained to generate the poses of the fibre placement head which is mounted at the robot manipulator's end-effector. Finally the simulation is carried out in software RobotStudio and the effect of laying is displayed using OpenGL. The simulation results verify the effectiveness of the proposed method.

Keywords—robotic fibre placement; path planning; triangular meshes

I. INTRODUCTION

Fibre reinforced composites play an important role in the aerospace and automotive industries because of their advantage of high strength-to-weight ratio, high stiffness-to-weight ratio, the thermal characteristics, low moisture absorption, etc. Nowadays, the application and the usage of the fibre reinforced composites have become an advanced sign of a new generation of aerospace crafts [1-3]. Robotic fibre placement is a widely used manufacturing technology for composite structures with low-cost, labor-saving and automation. It consists of a robotic manipulator, a placement head and a mould. The placement head is controlled by the robotic manipulator to lay down simultaneously a large number (up to 32) of the impregnated fibre tows. Then the tows are placed side by side on the mould surface. An elastomeric roller is used to place and compact the tows. By adopting a robot manipulator and multiple fibre tows, robotic fibre placement could make the composite structures with rapid manufacturing and mass production, and it can cut and restart each fibre tow to control the laying width which makes it suitable for complex structures with curvature changing significantly [4-6].

Path planning is one of key technologies within the scope of robotic fibre placement. It figures out the distribution of the fibre tows placed on the mould surface. The results of the path

planning directly determine the precision of the component forming and the efficiency of the placement. Much attention has been paid to this part and most path planning algorithms are mainly carried out on the mould expressed with parameter equation or mathematical expressions. A new path planning algorithm for open-contoured structures is proposed in [7]. In this method, the parametric equation of the mould surface is first given, then it uses a surface-plane intersection strategy to formulate the initial path. The next path is offset from the initial path along the surface by a distance with maximal tow-width in a perpendicular direction. Subsequent offset paths continue to be formulated until complete surface coverage is achieved. A varied offset distance method is developed to guarantee all the tows to be placed on the mould completely [8]. In their work, the roller location determination is taken into account, which allows a smooth roller motion along the generated path. The article [9] deduced an analytical algorithm about the path planning on the base of the mathematical model of the general revolved structures. In [10], a new parallel equidistant path generation algorithm based on the geodesic is introduced. This algorithm requires the distance between the paths equal along the geodesic direction. The following paths are achieved using the parallel equidistant algorithm until the mould surface is fully covered. However, it is inapplicable for most of the structures which are not expressed by parameter functions.

With the development of the three-dimensional measurement and the reverse modeling, the triangular mesh model is more and more widely used in the industrial fields of aerospace, automobile, shipbuilding mold which are closely related to the manufacturing industry. It has the advantage of rapid, flexibility and adaptable topology [11-12]. Articles [13-14] state path planning algorithms based on the meshed model, but the algorithms are mainly for the closed surface. Reference [15] presents a path planning algorithm for the open-contoured surface with isometric laying. The surface can be completely covered using this method. But for the airfoil open surface with the characteristic of the curve length of the two end sides are different, when laying angle is 90° , the fibre cutting concentrated on one side of the surface which could not ensure the component have enough compressive strength along the direction of 90° . It is necessary to place complete fibre tows connecting the root and the tip part regularly on every part of the surface, so a new path planning algorithm is proposed in the present work.

This work is supported in part by National Natural Science Foundation of China under grant 51405486.

The rest of this paper is organized as follows. The topology reconstruction of the meshed surface is introduced in section II. The path planning algorithm based on meshed surface is presented in section III. Section IV gives the implementation and verification of the algorithm. Simulations are given in section V. The paper is concluded in section VI.

II. TOPOLOGY RECONSTRUCTION OF THE MESHED SURFACE

In numeral control (NC) machining, the meshed surface data files are usually provided as Stereo Lithography (STL) model with saving three vertices of each triangular counterclockwise. In addition, the model used in rapid prototyping is often based on STL model which is a file with a large number of spatial triangular meshes being close to the original CAD entity model on the basis of minimizing geometric criterion. The discretization method of STL can satisfy the requirement of path planning based on meshed surface. That is where the surface curvature changing greatly the triangular mesh density is high and the mesh is sparse when the curvature with an even variation [16]. So the STL file of representing the mould surface is adopted.

The STL file is constituted by a lot of triangular meshes and each of which includes three-dimensional coordinates of three vertices and the normal vector of the mesh. The data redundancy of this file is large and it does not contain the topology among triangular meshes, the computation of path planning directly based on the STL file is very large. So, it is necessary to establish the topology of the STL format file, and remove the data redundancy. The surface topology reconstruction flow chart is shown in Fig. 1.

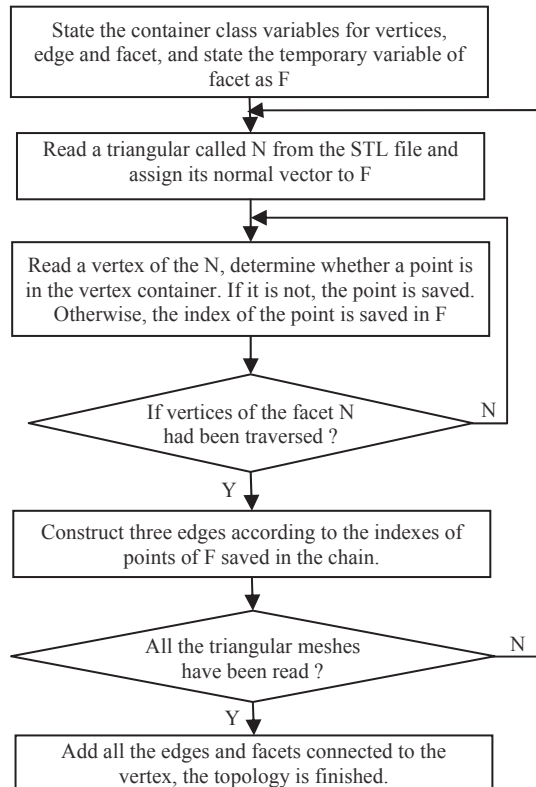


Fig.1 The diagram of the meshed surface topology reconstruction

After the topology reconstruction of the STL file, from a given facet, its three edges, three vertices and its normal vector can be easily obtained. From a known edge, its two vertices and two facets on its both sides can be achieved. Similarly, from a given vertex, its coordinate, all the edges and facets converged to it are also known from the topology.

III. THE PATH PLANNING ALGORITHM BASED ON THE MESHED SURFACE

Generally, the fibre tows are continually placed by the placement head at a certain angle which is often set as 0° , 90° , 45° , -45° respectively. The 0° is used to carry axial stress, the 90° is used to carry the radial stress, the 45° and -45° are used to carry shear stress. If the composite structure is under complex load, the layers of the structure are placed multidirectional according to the four angle types [17]. For the airfoil open surface, the curve length of the two end sides are different, a new path planning algorithm for robotic fibre placement is introduced.

A. The Generation of 0° Paths

The algorithm to generate 0° paths refers to the section contour in the process of slicing algorithm which is often used in rapid prototyping technology, and is one of the key contents of the software system of the rapid prototyping [18-19]. The length direction is set by the leading edge line which is shown in Fig. 2, the upper surface of the airfoil is where the fibre tows are placed. Slicing the airfoil open surface from the length direction along which the tangent plane can be expressed as $x = x_i$, where $i=1, 2, \dots, n$, and $x_{i+1} - x_i = D$, D is the maximal width during placing process where $D = d \times N_{\text{num}}$, d is the width of one fibre tow, N_{num} is the maximal number of fibre tows in the process of single laying.

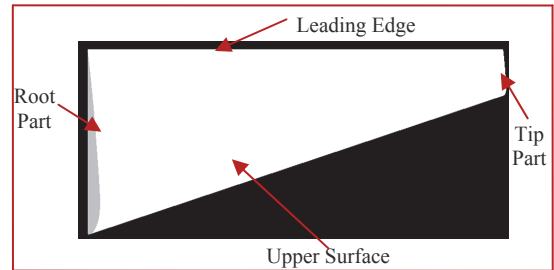


Fig.2 The airfoil model

Starting at the leading edge line, the edge of a triangular which intersects with the tangent plane but has not been sliced should firstly be found, then the point of intersection is computed, finally the coordinate of the point, the edge where the point locates and the facet which the point belonged to are saved. According to the topology, the next edge in the adjacent triangular which intersects with the tangent plane and also has not been sliced is found, the intersection point is also saved. The whole slicing data could be finally achieved in the same way.

B. The Generation of 45° Paths

When solving 45° paths, adopting the slicing direction as the reference line, the directions of 45° paths are got by rotating the reference line anticlockwise along the normal vector of the mesh where the path point locates, as shown in Fig. 3.

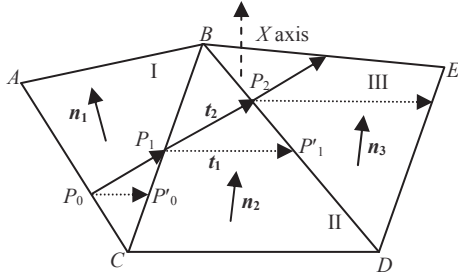


Fig.3 The diagram of path generation with 45°

In Fig. 3, \mathbf{n}_1 , \mathbf{n}_2 and \mathbf{n}_3 are normal vectors of the corresponding triangular meshes. Assuming P_1 is the start point of 45° path, the process of how to obtain trajectory point P_2 from P_1 is given as follows. Firstly, in the triangular mesh II, the point P_1' could be computed by the point P_1 on the basis of the slicing algorithm. The normal vector of the surface where point P_1 locates is the mean of the normal vectors of two adjacent triangular meshes with a common edge BC where the point P_1 locates, and is expressed as follows:

$$\mathbf{n}_{p1} = (\mathbf{n}_0 + \mathbf{n}_1)/2 \quad (1)$$

Taking the vector $\mathbf{P}_1\mathbf{P}_1'$ as vector \mathbf{t}_1 to represent the reference line, rotating \mathbf{t}_1 45° anticlockwise along \mathbf{n}_{p1} to get the vector \mathbf{t}_2 , the binormal vector \mathbf{k} of the surface where point P_1 locates is established as follows:

$$\mathbf{t}_2 = \text{Rot}(\mathbf{f}, \alpha) \cdot \mathbf{t}_1 \quad (2)$$

$$\mathbf{k} = \mathbf{n}_{p1} \times \mathbf{t}_2 = [x_k, y_k, z_k]^T \quad (3)$$

where

$$\text{Rot}(\mathbf{f}, \alpha) = \begin{bmatrix} f_x f_x \text{vers} \alpha + \cos \alpha & f_y f_x \text{vers} \alpha - f_z \sin \alpha & f_z f_x \text{vers} \alpha + f_y \sin \alpha \\ f_x f_y \text{vers} \alpha + f_z \sin \alpha & f_y f_y \text{vers} \alpha + \cos \alpha & f_z f_y \text{vers} \alpha - f_x \sin \alpha \\ f_x f_z \text{vers} \alpha - f_y \sin \alpha & f_y f_z \text{vers} \alpha + f_x \sin \alpha & f_z f_z \text{vers} \alpha + \cos \alpha \end{bmatrix} \quad (4)$$

$\mathbf{f}=[f_x, f_y, f_z]$ is the general rotation normal vector, f_x, f_y, f_z are the components of \mathbf{f} , and $\mathbf{f} = \mathbf{n}_{p1}$, $\alpha = 45^\circ$, $\text{vers} \alpha = 1 - \cos \alpha$.

The equation of the plane v constituted by the point $P_1(x_1, y_1, z_1)$ and the binormal vector \mathbf{k} could be expressed as follows:

$$x_k(x - x_1) + y_k(y - y_1) + z_k(z - z_1) = 0 \quad (5)$$

The edges of the triangular mesh II except BC where the current trajectory point P_1 locates could be evaluated as follows:

$$P(i) = (1-i)D + iB \quad (6)$$

where $D(x_d, y_d, z_d)$, $B(x_b, y_b, z_b)$ and $0 \leq i \leq 1$. By solving (5) and (6), the intersection point between the plane v and the line segment BD is expressed as follows:

$$i = \frac{x_k(x_1 - x_d) + y_k(y_1 - y_d) + z_k(z_1 - z_d)}{x_k(x_b - x_d) + y_k(y_b - y_d) + z_k(z_b - z_d)} \quad (7)$$

Therefore, the rules for obtaining the intersection point are listed below:

- If $0 < i < 1$, then the intersection point P_2 which is also the next trajectory point is between the two endpoints of the line segment BD , the coordinate of P_2 could be obtained from (6).
- If $i=0$ or $i=1$, then the intersection point is the endpoint of the line segment BD . Furthermore, if $i=0$, the next trajectory point $P_2=D$; if $i=1$, point $P_2=B$;
- If $i \notin [0,1]$, then substitute the last edge of triangular mesh II into (6), the parameter i is determined. Accordingly, if $0 \leq i \leq 1$, point P_2 can be computed similarly to the above two cases. Otherwise, traverse all the adjacent triangular meshes of point P_1 , each edge of the triangular is expressed by (6), then compute i until $i \in [0,1]$, and $\mathbf{P}_0\mathbf{P}_1 \cdot \mathbf{P}_1\mathbf{P}_2 > 0$, point P_2 is achieved finally.

When the trajectory point locates at the boundary of the model, just as P_0 in Fig. 3, the normal vector of where it locates is taken as the same with that of the triangular mesh I. If the point locates at the vertex of the triangular, as point P_i in Fig. 4, the normal vector of where it locates is defined as follows:

$$\mathbf{n}'_i = \frac{\sum_{k=1}^m s_k \mathbf{n}_{i,k}}{\sum_{k=1}^m s_k} \quad (8)$$

where $\mathbf{n}_{i,k}$ and s_k are the normal vector and the area of the adjacent triangular meshes of point P_i . The unit normal vector of point P_i is expressed as follows:

$$\mathbf{n}_i = \mathbf{n}'_i / |\mathbf{n}'_i| \quad (9)$$

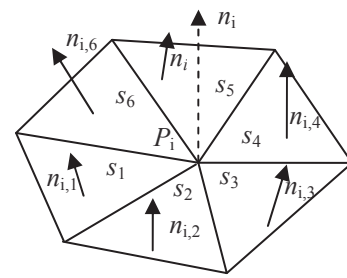


Fig.4 The neighborhood of the vertex P_i

C. The Generation of -45° Paths

The algorithm to get the -45° paths is similar with that to produce 45° paths. As in Fig. 3, taking the vector \mathbf{t}_1 as the reference line, the -45° paths are obtained by rotating \mathbf{t}_1 clockwise along the normal vector of the triangular where P_1 locates, and other steps are same with that in section B.

D. The Generation of 90° Paths

Because the curvature changes small on the upper surface of the airfoil, the fibre placement with maximal number of the fibre tows is carried out when the laying angles are 0°, 45°, -45°. Only at the surface boundary, the cutting and restarting information of fibre tows are needed to be known. However, when the laying angle is 90°, the arc lengths between the root part and the tip part are not equal, in order to ensure the component have enough compressive strength along the direction of 90°, it is required to place complete fibre tows from the root part to the tip part evenly on the surface. So an arc divided equally method is put forward to get the 90° paths.

Firstly, slicing the upper surface of the airfoil along the leading edge, contour curves which are numbered $\{L_1, L_2, L_3, \dots, L_m\}$ are achieved. The lengths of curves are computed, and the longest length is found. Supposing L_i is the longest one, dividing the length into n segments, and $n = \lceil L_i / (d \times N_{\text{num}}) \rceil$, where $\lceil \cdot \rceil$ is the round operator. Secondly, dividing other curves L_j (where $j = 1, 2, \dots, m$, and $j \neq i$) into n segments. Finally, connecting the corresponding point of every curve sequentially, the 90° paths are achieved.

IV. THE ALGORITHM IMPLEMENTATION

The method is implemented by C++ with the airfoil model as in Fig. 2. The 0° paths are got by the slicing algorithm, the $\pm 45^\circ$ paths are obtained by general rotation transformation, and an arc divided equally method is adopted to get the 90° paths.

A. The Implementation of Paths

The produced paths are displayed in Fig. 5, and four laying angles are 0°, 90°, 45°, and -45°.

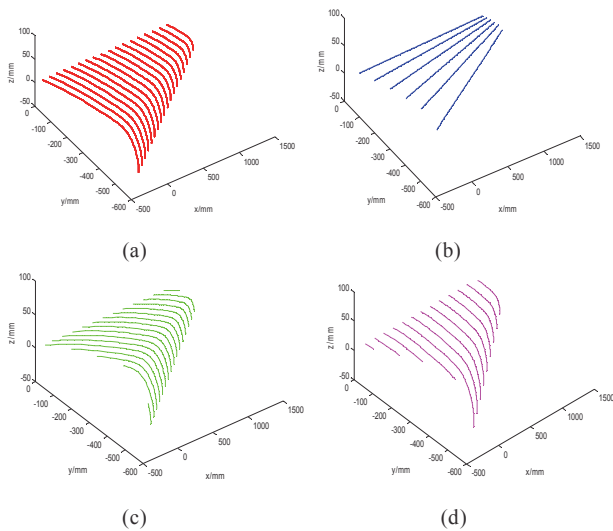


Fig.5 Planned paths with different angles, (a)0°, (b)90°, (c)45°, (d)-45°

B. Deleting redundant Path Points

The method of calculating path points is discussed in previous sections. The placement path is constituted by the serial connection of these path points. The above algorithm is experimented on the triangular meshes with the chord error is

0.3mm, the point density of each path is very high and the trajectory of the placement head is a set of line segments constituted by produced points, so it is necessary to delete the redundant path points for improving the laying efficiency. The maximal projection of the path points to the point connection line is defined as the step error ε , as shown in Fig. 6. With the step error $\varepsilon = 2.0\text{mm}$, the process of deleting redundant points are summarized as follows:

- Step 1: According to the moving forward direction of the placement head, supposing point $P_1=P_i$ as the start point, the coordinate of P_1 and the normal vector of where P_1 locates are saved, and if P_1 is the end point of the path, the computation stops. Otherwise, take point $P_2=P_{i+h}$ as the end point, where h is the number of points between them, and connect the two points to constitute the line L_i .
- Step 2: Compute the projection distances of every point between the start and the end point to the line L_i . Then find the maximal distance d_{max} .
- Step 3: If $d_{\text{max}} < \varepsilon$, set $h=h+1$, and return to step 2 until the inequality $d_{\text{max}} > \varepsilon$ is established for the first time, then set $h=h-1$. Otherwise, set $h=h-1$, and return to step 2 until the inequality $d_{\text{max}} \leq \varepsilon$ is achieved for the first time.
- Step 4: Point P_{i+h} is taken as the next path points and coordinate and normal vector of P_{i+h} are also saved. Then set $P_1=P_{i+h}$ as the start point, return to step 2. If P_{i+h} is the end point of the path, the computation stops.

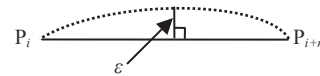


Fig.6 The step error ε neighborhood of the vertex

On the basis of meeting the step error requirement, the number of path points decrease obviously, as illustrated in table 1. The reduced points can improve the efficiency of the fibre placement.

TABLE I. THE NUMBER OF PATH POINTS

Laying Angle	The Number of Path Points	
	The Initial Num	The End Num
0°	80	19
90°	142	2
45°	80	21
-45°	80	21

V. SIMULATION

A. Simulation in Software Robotstudio

During the placement process, the path points are finally used to generate the poses of the placement head which is on the end-effector of robot. ABB IRB6640 robot is adopted as

the placement robot, the pose of the placement head is solved from the following equation:

$${}^W T_E \cdot {}^E T_D = {}^W T_O \cdot {}^O T_P \quad (10)$$

where T is the rotation transformation matrix, W is the world coordinate system, E is the coordinate system of the tool center point (TCP) of robot, D is the tool coordinate system of the placement head, O is the workpiece coordinate system, P is the path point. ${}^W T_E$ is the rotation matrix from E to W , ${}^E T_D$ is the rotation matrix from D to E , ${}^W T_O$ and ${}^O T_P$ are also rotation matrix from O to W and P to O separately.

Firstly, assuming the rotation matrix of the placement head at path points as $[\mathbf{n} \ \mathbf{o} \ \mathbf{a}]$, where $\mathbf{a} = -\mathbf{k}$ to guarantee that the direction of the placing by placement head is reverse to \mathbf{k} which is the normal vector of the surface. The connection of the two adjacent points is set as the forward laying:

$$\mathbf{n} = (x_2 - x_1, y_2 - y_1, z_2 - z_1) / \|(x_2 - x_1, y_2 - y_1, z_2 - z_1)\| \quad (11)$$

where (x_1, y_1, z_1) and (x_2, y_2, z_2) are coordinates of two adjacent path points. Setting $\mathbf{o} = \mathbf{n} \times \mathbf{a} / \|\mathbf{n} \times \mathbf{a}\|$, and then \mathbf{n} is revised as $\mathbf{n} = \mathbf{o} \times \mathbf{a}$ for ensuring the coordinate system to be orthogonal. The general rotation transformation matrix ${}^O T_P$ is expressed as follows:

$${}^O T_P = \begin{bmatrix} n_x & o_x & a_x & x \\ n_y & o_y & a_y & y \\ n_z & o_z & a_z & z \\ 0 & 0 & 0 & 1 \end{bmatrix} \quad (12)$$

where (x, y, z) is the coordinate of the path point. The matrix ${}^W T_O$ is established as follows:

$$\begin{aligned} {}^W T_O &= \text{rot}(Z, \alpha) \text{Trans}(d_1, d_2, d_3) \\ &= \begin{bmatrix} \cos \alpha & -\sin \alpha & 0 & 0 \\ \sin \alpha & \cos \alpha & 0 & 0 \\ 0 & 0 & 1 & 0 \\ 0 & 0 & 0 & 1 \end{bmatrix} \begin{bmatrix} 1 & 0 & 0 & d_1 \\ 0 & 1 & 0 & d_2 \\ 0 & 0 & 1 & d_3 \\ 0 & 0 & 0 & 1 \end{bmatrix} \quad (13) \end{aligned}$$

where $\alpha = -90^\circ$ is the mould rotation angle along the z axis, $[d_1, d_2, d_3] = [1500, 0, 1000]^T$ mm is the translation vector of the mould in the world coordinate system. Taking ${}^E T_D = E$ for simplification, the pose of the placement head in the world coordinate system could be got. However, the pose is expressed by quaternion $[q_1, q_2, q_3, q_4]$ in the controller of ABB robot, it is necessary to convert the pose which is expressed by rotation matrix to quaternion. The quaternion is given by the following equation:

$$\begin{cases} q_1 = \sqrt{n_x + o_y + a_z + 1} / 2 \\ q_2 = \text{sign}(o_z - a_y) \sqrt{n_x - o_y - a_z + 1} / 2 \\ q_3 = \text{sign}(a_x - n_z) \sqrt{o_y - n_x - a_z + 1} / 2 \\ q_4 = \text{sign}(n_y - o_x) \sqrt{a_z - n_x - o_y + 1} / 2 \end{cases} \quad (14)$$

The simulation of fibre placement is carried out in RobotStudio which is ABB robot simulation software. Taking the 0° paths for example, the simulation is shown in Fig. 7.

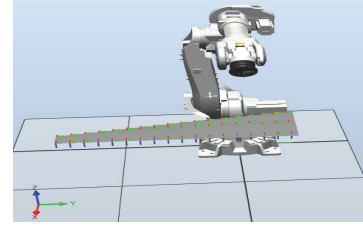


Fig.7 The simulation of paths with the angle of 0°

As shown in Fig. 7, x direction is the laying direction of the placement head, z direction is perpendicular to the mould surface downward. The simulation results indicate that the fibre tows could be placed uniformly on the mould surface by the placement head with a certain pose.

B. The Displacement of the Laying Effect

After the simulation in RobotStudio with angles of 0° , 45° , 90° , -45° is done, the laying effects are displayed in OpenGL as shown in Fig. 8 as follows:

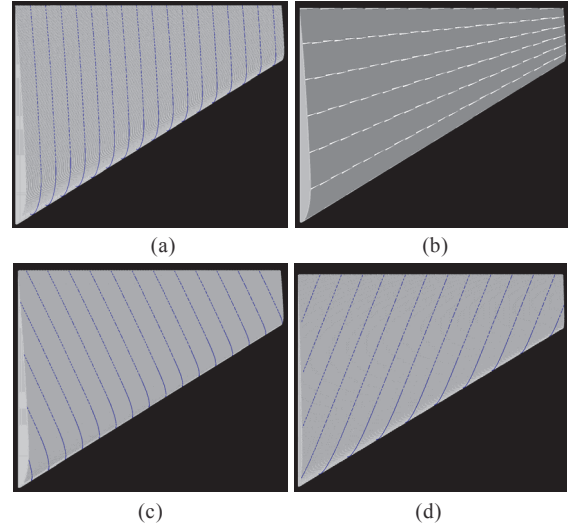


Fig.8 The laying effect with different angles, (a) 0° , (b) 90° , (c) 45° , (d) -45°

The effect of laying with the angle of 0° is shown in Fig. 8(a). 0° paths are obtained by slicing algorithm along the leading edge of the airfoil and the width of the fibre is D , where $D = d \times N_{\text{num}} = 102.4\text{mm}$, $d = 3.2\text{mm}$, and $N_{\text{num}} = 32$. The blue dotted lines are the boundary of fibre ribbon. For 45° paths, as in Fig. 8(c), the distance between two adjacent fibre ribbons along the leading edge is H , where $H = \sqrt{2}D = 144.8\text{mm}$. The -45° paths in Fig. 8(d) have the similar character with 45° paths.

Fig. 8(b) shows the laying effect of 90° paths which are produced by an arc divided equally method. Because each fibre tow has a certain width, and it has to be cut off the total width when the cut is needed. So the gap is produced inevitably. The white blocks state the gaps during the placement. The coefficient f ($0 \leq f \leq 1$) can be set to control the gap and overlap during the placement. If $f = 0$, the gap is the maximum without overlap and if $f = 1$, the overlap is largest

without gap just as shown in Fig. 9. During laying process, by adjusting the coefficient f , the percentage of the overlap and gap could be manipulated to avoid excessive gap and too much overlap which could improve the performance of the forming structure.

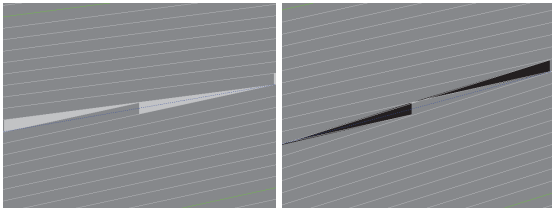


Fig.9 The laying effect with $f=0$ and $f=1$

VI. CONCLUSION

In this paper, a new path planning algorithm for airfoil open surface is presented with commonly used laying angles of 0° , 90° , 45° , -45° . The proposed method formulates a serial of path points which meet the step error requirement. The simulation is well conducted in software RobotStudio and the placement effect is displayed by OpenGL. The results of simulation show that the fibre tows could be placed on the mould surface evenly without gap and overlap when the laying angles are 0° , 45° , -45° . When the laying angle is 90° , the relationship between the gap and overlap could be controlled by adjusting the coefficient f . The paths generated by the proposed method all meet the technological requirement of the fibre placement.

ACKNOWLEDGMENT

The research is supported by the Research Center of Precision Sensing and Control, Institute of Automation, Chinese Academy of Sciences.

REFERENCES

- [1] G. Marsh, "Automating aerospace composites production with fibre placement," *Reinforced Plastics*, vol. 55, no. 3, 2011, pp. 32-37.
- [2] P. Debout, H. Chanal, and E. Duc, "Tool path smoothing of a redundant machine: Application to Automated Fiber Placement," *Computer-Aided Design*, vol. 43, no. 2, 2011, pp. 122-132.
- [3] M. Bruyneel and S. Zein, "A modified fast marching method for defining fiber placement trajectories over meshes," *Computers and Structures*, vol. 125, no. 1, 2013, pp. 45-52.
- [4] B. Shirinzadeh, G. Alici, and C. W. Foong, "Fabrication process of open surfaces by robotic fibre placement," *Robotics and Computer-Integrated Manufacturing*, vol. 20, no. 1, 2004, pp. 17-28.
- [5] J. Xiao, Y. Li, and J. L. Li, "The application of automatic fiber placement in manufacture of composite structures in large aircraft," *Aeronautical Manufacturing Technology*, vol. 1, no. 1, 2008, pp. 50-53.
- [6] Q. G. Xue, "Efficient and automatic fiber placement equipment of carbon fiber composite materials," *Aeronautical Manufacturing Technology*, vol. 1, no. 4, 2008, pp. 20-24.
- [7] B. Shirinzadeh, G. Cassidy, and D. Oetomo, "Trajectory generation for open-contoured structures in robotic fibre placement," *Robotics and Computer-Integrated Manufacturing*, vol. 23, no. 4, 2007, pp. 380-394.
- [8] L. Yan, Z. C. Chen, and Y. Shi, "An accurate approach to roller path generation for robotic fibre placement of free-form surface composites," *Robotics and Computer-Integrated Manufacturing*, vol. 30, no. 3, 2014, pp. 277-286.
- [9] W. Zeng, J. Xiao, and Y. Li, "Research on path planning and coverability analysis of automatic fiber placement for structures in revolving shell," *Journal of Astronautics*, vol. 1, no. 1, 2010, pp. 239-243.
- [10] X. D. Dang, J. Xiao, and D. J. Huan, "Implementation on fiber placement parallel equidistant path generation algorithm," *Journal of Wuhan University(Natural Science Edition)*, vol. 53, no. 5, 2007, pp. 613-616.
- [11] J. T. Xu, W. J. Liu, and H. Y. Bian, "Constant scallop tool path for triangular surface machining," *Journal of Mechanical Engineering*, vol. 46, no. 11, 2010, pp. 193-198.
- [12] Y. W. Sun, D. M. Guo, and Z. Y. Jia, "Iso-parametric tool path generation from triangular meshes for free-form surface machining," *The International Journal of Advanced Manufacturing Technology*, vol. 28, no. 7, 2006, pp. 721-726.
- [13] W. L. Xiong, J. Xiao, and X. F. Wang, "Algorithm of adaptive path planning for automated placement on meshed surface," *Acta Aeronautica ET Astronautica Sinica*, vol. 34, no. 2, 2013, pp. 434-441.
- [14] J. F. Li, X. F. Wang, and J. Xiao, "Trajectory planning of automated fiber placement for meshed surface in fixed angle algorithm," *Journal of Computer-Aided Design & Computer Graphics*, vol. 25, no. 9, 2013, pp. 1410-1415.
- [15] V. D. Holla, K. G. Shastry, and B. G. Prakash, "Offset of curves on tessellated surfaces," *Computer-Aided Design*, vol. 35, no. 12, 2003, pp. 1099-1108.
- [16] Y. W. Sun, J. Liu, and W. J. Liu, "Reconstructing accurate boundary representation from STL model," *Journal of Computer-Aided Design & Computer Graphics*, vol. 16, no. 7, 2004, pp. 944-949.
- [17] L. L. An, Y. Zhou, and L. S. Zhou, "Composite fiber placement path planning and fiber number determination," *Acta Aeronautica ET Astronautica Sinica*, vol. 28, no. 3, 2007, pp. 745-750.
- [18] B. J. Zhao, S. Wang, and W. Y. Chen, "Algorithm for rapid slicing STL model," *Journal of Beijing University of Aeronautics and Astronautics*, vol. 30, no. 4, 2004, pp. 329-333.
- [19] X. D. Jiao, S. C. Deng, and P. Zhang, "Rapid Prototyping Based on Robotic Gas Arc Metal Welding," *Robot*, vol. 23, no. 7, 2001, pp. 657-660.